



Sulfur Poisoning and Regeneration of Ni-Based Anodes in Solid Oxide Fuel Cells

Shaowu Zha,* Zhe Cheng,** and Meilin Liu*^z

School of Materials Science and Engineering, Georgia Institute of Technology Atlanta,
Georgia 30332-0245, USA

The effect of hydrogen sulfide (H₂S) on the performance of nickel/yttria-stabilized zirconia (YSZ) cermet anode for solid oxide fuel cells has been studied under various operating conditions. In all cases, a small amount of H₂S (ppm level) causes a sharp drop in cell performance within the first few minutes of exposure, followed by a gradual but persistent deterioration in performance for several days. The extent of anode degradation caused by sulfur poisoning increases with increasing H₂S concentration, increasing cell voltage (i.e., closer to open-circuit voltage or decreasing cell current density), or decreasing cell operating temperature. The initial sharp degradation in performance is attributed to rapid adsorption of sulfur onto the Ni surface, which blocks the active sites for hydrogen adsorption and oxidation. However, the mechanism for the subsequent slow degradation is still not clear. Upon removal of H₂S from the fuel stream, the anode performance can be recovered fully or partially, depending on operating conditions and duration of H₂S exposure. The rate of the recovery process increases with operating temperature and cell current density. © 2006 The Electrochemical Society. [DOI: 10.1149/1.2404779] All rights reserved.

Manuscript submitted February 6, 2006; revised manuscript received October 2, 2006.
Available electronically December 22, 2006.

Solid oxide fuel cells (SOFCs) have great potential for direct utilization of hydrocarbon fuels, including hydrogen-rich synthesis fuels derived from coal or natural gas.¹⁻³ This would eliminate the need for a separate fuel processing subsystem and reduce the cost and complexity of SOFC system. Unfortunately, all fossil fuels contain some amounts of contaminants such as sulfur compounds. In reforming, the sulfur compounds are converted to gaseous hydrogen sulfide (H₂S). The nickel-based anodes for current SOFC have very limited tolerance to H₂S: significant poisoning was observed if the H₂S concentration was above 5–10 ppm at 950–1000°C.⁴⁻⁸ In addition, for the same H₂S level, the extent of sulfur poisoning increases dramatically as the operating temperature is decreased from 1000°C to lower temperatures.^{4,8} As a result, the H₂S concentration in the feed fuel usually must be reduced to less than 0.2 parts per million by volume (ppmv).⁹ In recent years, considerable efforts have been devoted to studying the sulfur poisoning process of the Ni-based anodes of SOFC^{4-8,10,11} and the development of sulfur-tolerant anode materials.¹²⁻²¹ To date, however, the reported sulfur poisoning behavior is not consistent in the literature and a detailed understanding of the sulfur-anode interaction mechanism under fuel cell operating conditions is still lacking. Some researchers proposed that the sulfur poisoning of the anode is caused by formation of conventional bulk nickel sulfides (e.g., Ni₃S₂) upon exposure to H₂S, which block the catalytic sites of Ni along the triple-phase boundaries (TPBs) and results in the performance degradation. However, thermodynamic analysis suggests that bulk nickel sulfides will decompose to metallic nickel and H₂S when the $p_{\text{H}_2\text{S}}/p_{\text{H}_2}$ ratio is below $\sim 10^{-3}$ at temperatures greater than $\sim 700^\circ\text{C}$.^{10,22,23} Other researchers proposed that the poisoning is due to sulfur adsorption on the surface of Ni, which is also consistent with the fact that surface nickel sulfides (viz., adsorbed sulfur on Ni) are significantly more stable than bulk nickel sulfides under low surface coverage condition (see the review by Bartholomew et al.²⁴ for more details).

Note that most of the previous studies on sulfur poisoning of catalysts were focused on chemical reactions (e.g., steam reforming, hydrocarbon hydrogenation and methanol synthesis) instead of fuel cell (electrochemical) reactions.²⁴ Unlike chemical catalysis, additional electrochemical processes take place at the anode of an SOFC because of the anodic polarization and oxygen ion flow to anode from cathode through the electrolyte under fuel cell operation. Accordingly, sulfur poisoning of the anode of an SOFC is more complicated. In this study, we investigated the effect of H₂S on cell

performance and interfacial resistance for a single SOFC with Ni-YSZ cermet anode under different operating conditions (i.e., temperature, H₂S concentration and cell voltage/current) using dc polarization techniques and impedance spectroscopy. The recovery in cell performance after the fuel was switched back to clean hydrogen was also studied.

Experimental

Preparation of single SOFCs.—(ZrO₂)_{0.92}(Y₂O₃)_{0.08} powder (YSZ, TZ-8Y, Tosoh) was cold-pressed at ~ 75 MPa into cylindrical pellets using a uniaxial die-press, followed by sintering at 1500°C for 5 h to obtain dense YSZ disks with thickness of ~ 0.25 mm. One side of the YSZ pellets was coated with NiO-YSZ anode material (Ni:YSZ volume ratio is 60:40 after reduction) and fired at 1450°C for 2 h. A cathode slurry consisting of strontium doped lanthanum manganite (La_{0.85}Sr_{0.15}MnO₃, LSM, Rhodia) and organic binder was then painted onto the opposite side of the YSZ disk and fired at 1250°C in air for 2 h. A thin layer of platinum paste was painted on the cathode side. Platinum mesh and wire (Alfa Aesar) were attached to both electrodes as current collectors. No Pt paste was applied to the anode surface.

Characterization of sulfur poisoning and regeneration processes.—Schematically illustrated in Fig. 1 is the experimental apparatus for testing a single SOFC. The button cell was mounted onto an alumina tube and sealed with ceramic adhesive (Autostic FC-6, Flexbar). The cathode side was open to the ambient air. In the case of 50 ppm H₂S, pure H₂ and humidified N₂, each flowing at 10 mL/min were mixed and passed through the test setup (nominal fuel composition is 50% H₂/1.5% H₂O/48.5% N₂); then fuel with 50 ppm H₂S was obtained by replacing the pure H₂ flow with a certified gas mixture of 100 ppm H₂S in H₂ (Airgas) at the same flow rate (nominal fuel composition is 50 ppm H₂S/50% H₂/1.5% H₂O/48.5% N₂). (The 100 ppm H₂S/H₂ gas mixture was not passed through water bubbler because H₂S could dissolve in water, which would delay the observed response of the cell.) In the case of 0.18–10 ppm H₂S, the H₂S concentration was adjusted by mixing pure H₂ and certified mixture gas of 10 ppm H₂S in H₂ (Airgas) using two mass flow controllers (Omega Engineering Inc.). The total flow rate was also 20 mL/min. The gas line volume from the H₂S valve to the anode surface is as little as ~ 6 mL. Such small idle volume has two benefits—the H₂S gas can reach the anode quickly, and a very short time is required to sweep away residual H₂S when the fuel was switched back to clean H₂.

The extent of sulfur poisoning was measured as a function of H₂S concentration, total H₂S exposure time, cell temperature and

* Electrochemical Society Active Member.

** Electrochemical Society Student Member.

^z E-mail: meilin.liu@mse.gatech.edu

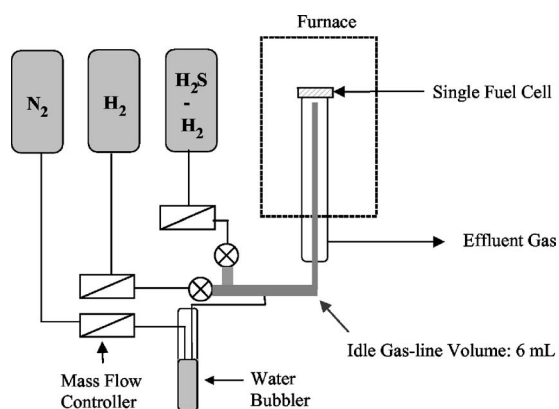


Figure 1. Schematic illustration of the setup for fuel cell testing.

operating voltage/current. To examine the reversibility of the poisoning effect, the cell was “regenerated” by flowing H_2S -free fuel to the anode chamber. The fuel cell performance was measured using an EG&G potentiostat/galvanostat (273A, Princeton Applied Research) controlled by software. While both potentiostatic (i.e., constant cell voltage) and galvanostatic mode (i.e., constant cell current) can be used for cell performance testing, most of the experiments were carried out using the potentiostatic mode to avoid possible catastrophic damage to the cell due to dramatic sulfur poisoning under galvanostatic mode when the initial cell voltage is lower than half of the open circuit voltage. Impedance responses of fuel cells under open-circuit conditions were measured in the frequency range from 100 kHz to 0.01 Hz using an EG&G lock-in amplifier and an EG&G potentiostat/galvanostat interfaced with a computer.

Results and Discussion

Fuel cell performance and stability in H_2 .—Figure 2 shows the cell voltage and power density as a function of current density for a typical single SOFC fabricated in this study. The cell performance is moderate, considering the cell is electrolyte-supported with an electrolyte thickness of ~ 0.25 mm. As is demonstrated later, both sulfur poisoning and subsequent regeneration processes are strongly affected by the current density passing through the cell. Therefore, the fuel cell fabrication and testing conditions were kept as identical as possible to obtain repeatable performance.

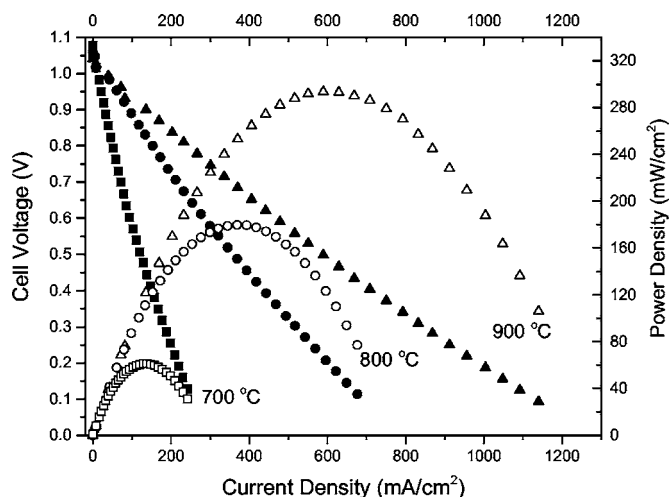


Figure 2. Cell voltage and power density as a function of current density for a typical Ni-YSZ/YSZ/LSM fuel cell running on H_2 - N_2 fuel.

To determine the impact of H_2S poison on the anode, especially in the long-term, it is imperative to ensure stable cell performance in hydrogen fuel. Figure 3 shows the typical performance of a cell operated at a constant cell terminal voltage in fuel of 50% H_2 /1.5% H_2O /48.5% N_2 . The performance of the cell increased and then stabilized after running at 0.6 V for 96 h at 900°C. After that, the cell temperature was decreased to 800°C and the cell maintained a constant power output for another 120 h. The initial increase in cell performance was attributed to cathode conditioning (activation), as observed by many researchers during the initial period of cell operation.²⁵⁻²⁸ It was also found that lower cell current led to longer time for the cell performance to stabilize. As a result, all fuel cells tested in this study were stabilized at cell voltage of 0.7 V at 900°C for >90 h before characterizing the sulfur poisoning effect.

Time dependence of H_2S poisoning and regeneration processes.—Figure 4a shows representative sulfur poisoning and recovering processes of a single SOFC with Ni-YSZ cermet anode upon exposure to a fuel containing 50 ppm H_2S under constant cell voltage. The poisoning process appeared to have two stages: a dramatic drop (-16.67%) in cell current occurred in the first several minutes followed by a slow but continuous performance drop (up to -3.96%) in the next 120 h. Upon removal of H_2S from the fuel, the cell performance first had a quick rebound then recovered gradually. (The downward spike at ~ 145 h was due to fluctuation in flow rate upon the gas switch.) The recovery was not complete and the cell performance stabilized at $\sim 96\%$ of the initial value after 50 h. Similar to the results in fuel with 50 ppm H_2S , a dramatic performance drop followed by a slow and continuous degradation was also observed when the anode was exposed to a fuel mixture with 2 ppm H_2S , as shown in Fig. 4b. Compared to the poisoning effect of 50 ppm H_2S , the extent of degradation caused by 2 ppm H_2S was smaller with an initial degradation of 12.67% and the recovery process was faster and more complete (the cell performance stabilized to $\sim 99\%$ of the initial value). These results suggest the sulfur poisoning effect is accumulative and becomes more severe with increasing H_2S concentration and exposure time. Indeed, performance degradation after a brief exposure to H_2S can be fully recovered in a short time. As shown in Fig. 4c, a cell was exposed to 2 ppm H_2S for 6 min and the cell performance recovered fully after clean H_2 was flown for ~ 40 min. These observations suggest that in a real SOFC system, a short leakage of H_2S for several minutes can be tolerated and will not cause irrecoverable damage.

The observed two-stage poisoning/recovery behavior is similar to that reported by Singhal et al.⁴ Note, however, that they observed full recovery in fuels with 2–10 ppm H_2S at 1000°C under constant current conditions. Our cells were operated in fuels with higher concentration of H_2S (2–50 ppm at 700–900°C) at lower temperatures. Our observation is also somewhat similar to the initial poisoning behavior (in the first 1000 sec) observed by Sasaki et al. for Ni-YSZ anode in a fuel with 20 ppm H_2S at 800°C at a constant cell current of 200 mA/cm².¹⁰ However, several significant differences are noted in these studies. First, the sulfur poisoning for Sasaki’s cell with Ni-YSZ anode is much more severe and faster (i.e., 75% degradation in ~ 1000 s) than that of our cells, which is not easy to explain as the cell performances are comparable with each other (250 mA/cm² at 0.6 V for Sasaki’s cell versus 0.7 V at 200 mA/cm² for cells in this study). Second, Sasaki’s cell with Ni-YSZ anode also displayed a third stage of sulfur poisoning: the performance degradation accelerated again after ~ 1000 sec at cell voltage of ~ 0.18 V and failed quickly at ~ 1500 sec. This might be related to the very low cell voltage, which could incur oxidation of the Ni anode and drive the current to zero. Such failure was never observed in our study. Third, the multi-stage poisoning process that Sasaki observed for Ni- Sc_2O_3 stabilized ZrO_2 (SSZ) cermet anode is also difficult to explain, but it is still very interesting to observe that changing the electrolyte component in the cermet from YSZ to SSZ would have such huge effect on the sulfur poisoning behavior of the anode. No induction time was observed in this study and the cell

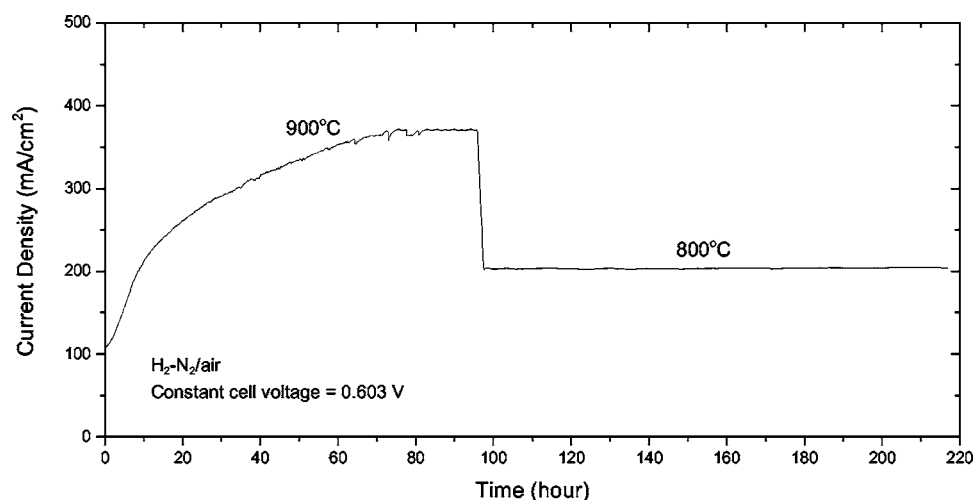


Figure 3. Changes in cell current density vs time for a single SOFC operated at a constant cell voltage of 0.6 V for 9 days. The cell was operated at 900°C for the first 96 h, and then cooled down to 800°C and kept running for another 120 h.

performance dropped as soon as H_2S was introduced into the fuel stream, which is different from the result by Xia and Birss who observed that their cell started to degrade after 10 ppm H_2S had been introduced into the fuel flow for $\sim 1\text{--}2$ h.¹¹

Influence of H_2S concentration and temperature.—Figure 5 shows the dependence of cell performance degradation on H_2S concentration at temperatures from 700 to 900°C. All data was collected based on change in cell current after H_2S was introduced for 5 min (i.e., just after the first stage of sulfur poisoning) for cells operated at a constant voltage. The fuel cell performance degraded even when the H_2S concentration was as low as 0.18 ppm. At a given temperature, the extent of sulfur poisoning increased with increasing H_2S

concentration in the fuel. For a given concentration of H_2S , the poisoning effect was more severe at lower temperature. Such a trend is reasonable as higher H_2S concentration leads to higher equilibrium coverage for sulfur adsorbed on nickel while lower temperature generally lead to slower desorption rate and higher equilibrium coverage. It also agrees with the results (measured under constant current condition) by Singhal et al.⁴ The data shown in Fig. 5 represent the effect of temperature and H_2S concentration on the sulfur poisoning behavior of a SOFC with the state-of-the-art anode material.

Influence of cell voltage.—Figure 6 shows the change in current density for cells operated under different cell voltage at 800°C in

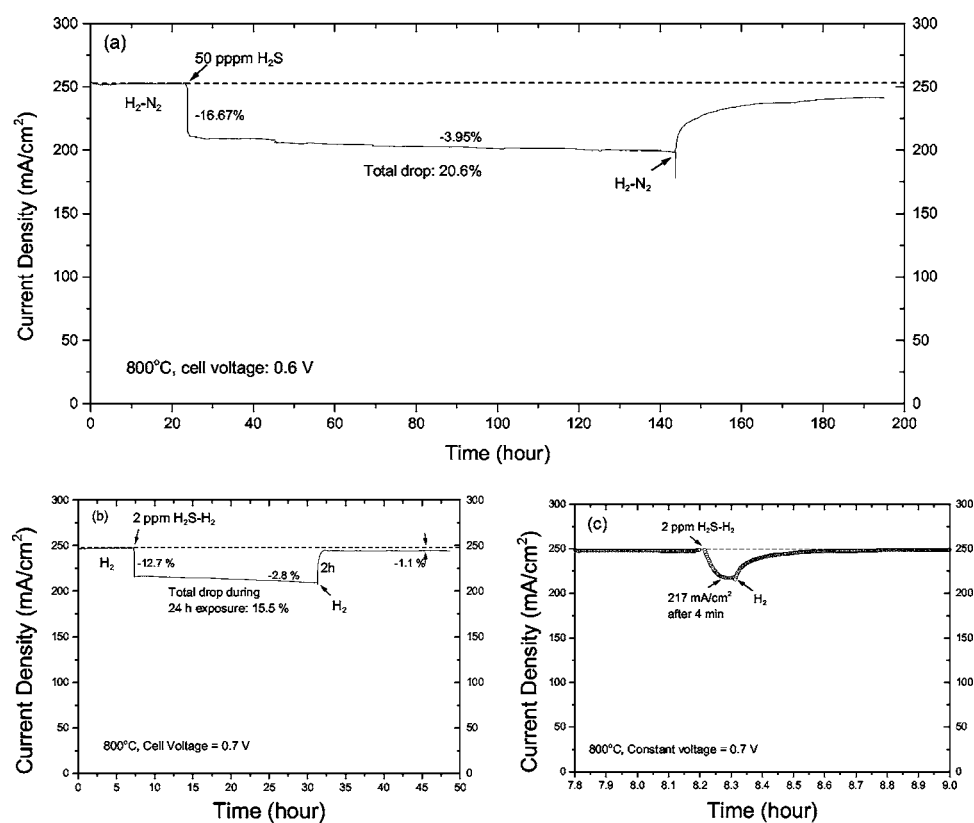


Figure 4. Sulfur poisoning and regeneration (or desulfurization) processes of Ni-YSZ anodes in a fuel mixture with (a) 50 ppm and (b and c) 2 ppm H_2S .

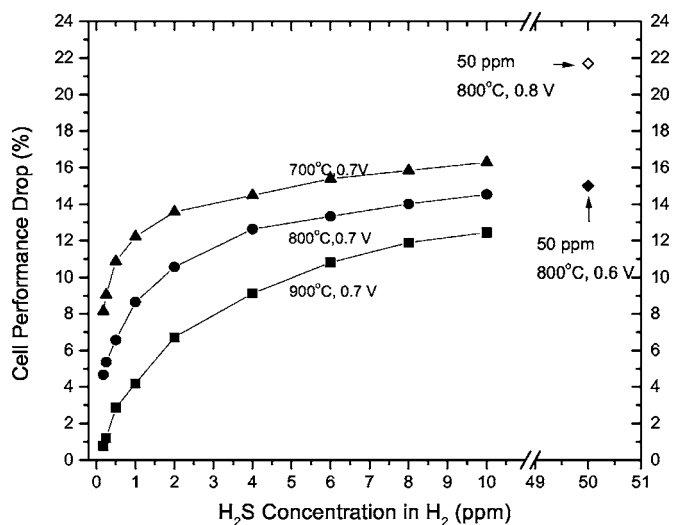


Figure 5. Dependence of cell performance drop (measured in terms of percentage change in current density under a constant voltage) on H₂S concentration at different temperatures.

fuels with and without 50 ppm H₂S. Both the sulfur poisoning and subsequent regeneration processes depend strongly on cell operating voltage. The extent of sulfur poisoning decreased from 32.3% to 15.5% when the cell terminal voltage was decreased from 0.8 V (or cell current density of ~ 120 mA/cm²) to 0.3 V (or cell current density of ~ 510 mA/cm²); the cell recovered to 99.5% of the original level at cell voltage of 0.3 V (~ 510 mA/cm²) while it recovered to only 89.5% of the original level at cell voltage of 0.8 V (~ 120 mA/cm²). It appears that the current passing through the cell might help the electrochemical oxidation of the sulfur adsorbed on Ni surfaces to SO₂ near the TPB. Once sulfur is oxidized to SO₂, it will quickly desorb from anode surface, leading removal of sulfur from anode surfaces. However, the cell voltage or cell current density does not seem to have observable effect on the rate of sulfur poisoning.

Impedance spectroscopy.— Shown in Fig. 7 are the impedance spectra of functional fuel cells measured using two-electrode configuration before and after the anodes were exposed to fuels containing 1 ppm H₂S at 800, 850, and 900°C, respectively. At each temperature, the bulk resistance (R_{Ω}) remained the same while the interfacial resistance increased dramatically after the anode was exposed to H₂S-containing fuel. Qualitative examination of the impedance spectra indicates that each impedance spectrum appears to consist of three arcs (marked as Z₁, Z₂, Z₃ in the plot for 800°C), each at a different range of frequencies noted as high (HF), intermediate (IF) and low frequency (LF), respectively. It seems that the high and low frequency arcs, Z₁ and Z₃, remained essentially the same whereas Z₂ became significantly larger upon exposure to a H₂S contaminated fuel. Thus, Z₂ appears to be associated with the sulfur poisoning processes.

Shown in Fig. 8a are the impedance spectra of a fuel cell acquired under open-circuit conditions using two-electrode configuration when the anode was exposed to hydrogen containing different concentrations of H₂S at 800°C. In all cases, the “shapes” of the impedance spectra are similar to those shown in Fig. 7. The bulk resistance of the electrolyte (R_{Ω}) was unchanged before and after exposure to H₂S. The arcs at HF and LF, corresponding to the cathodic interfacial polarization resistance and mass transfer limitation, are relatively independent of the concentration of H₂S. However, the arcs at IF, corresponding to the polarization resistance of the anode-electrolyte interfaces, increased significantly when 1 ppm H₂S is added to the fuel gas; it increased even more with increasing

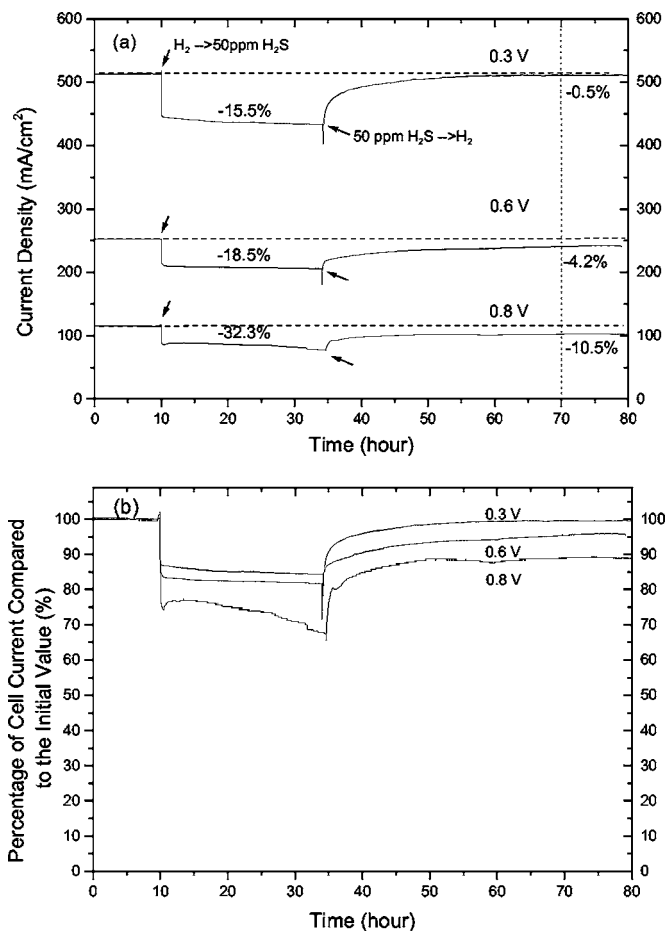


Figure 6. Influence of cell voltage on the poisoning and regeneration processes for three functional SOFCs at 800°C: (a) Plots of cell current densities as a function of time at various cell voltages, 0.3, 0.6, and 0.8 V, respectively. 0–10 h, 34–80 h: Fuel = 50% H₂/1.5% H₂O/48.5% N₂; and 10–34 h: Fuel = 50 ppm H₂S/50% H₂/1.5% H₂O/48.5% N₂, Flow rate = 20 mL/min. The percentage numbers on the vertical dash line shows the uncovered current drops after flowing clean H₂ fuel for 26 h. (b) Plots of percentages of cell current drops as a function of time at various cell voltages.

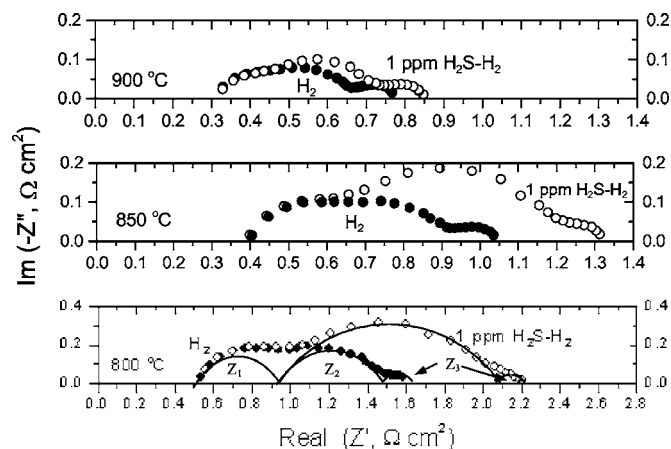


Figure 7. Impedance spectra of functional fuel cells measured using two-electrode configuration under open-circuit conditions before and after introducing 1 ppm H₂S to the anodes at 800, 850, and 900°C, respectively.

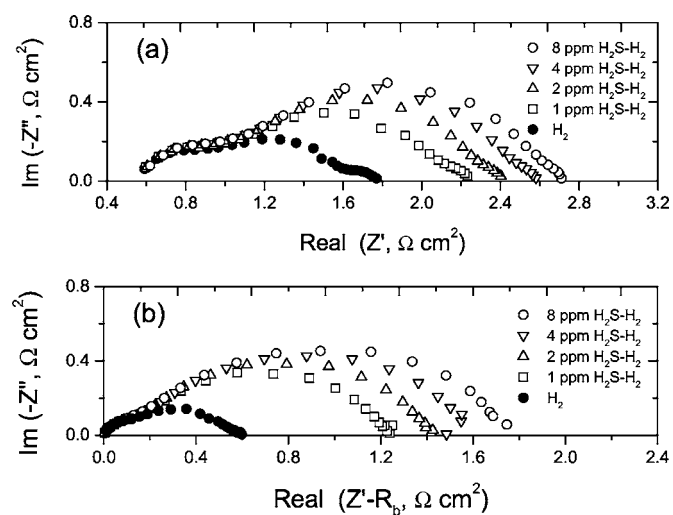


Figure 8. Impedance spectra measured under open-circuit conditions (a) for a full cell using a two-electrode configuration and (b) for anode/electrolyte interface using three-electrode configuration.

H_2S concentration up to 8 ppm. Figure 8b shows the change in anode/electrolyte interfacial resistance measured under OCV with three-electrode configuration. The anode/electrolyte interfacial resistance accounts for one-third of the total cell resistance, and it is clear that the anode interfacial resistance increased dramatically (up to $\sim 200\%$) when it was exposed to fuels with trace amount of H_2S . Such behavior was consistent with the conclusion obtained by Matsuzaki and Yasuda⁸ who studied the change in impedance for a cell with cermet electrode containing 86 vol % Ni and a Pt counter electrode in a single chamber. It is also consistent with the observed changes in cell current shown before and agrees with the observations made by other researchers.^{5,6,11}

Figure 9 shows the change in anode/electrolyte polarization resistance on a percentage base for a cell operated at 800°C measured under open-cell voltage (OCV) and estimated under constant cell voltage of 0.7 V (with the assumption that anode polarization resistance constitutes one-third of the total dc resistance). The plot clearly shows the dramatic decrease in anode activity caused by H_2S . For the same H_2S concentration, the poisoning is more severe at OCV (no current flow) than under a load (with a finite current flowing through the cell), indicating that the current passing through the cell might help the removal of the sulfur adsorbed on anode surfaces by electrochemical oxidation of sulfur to SO_2 .

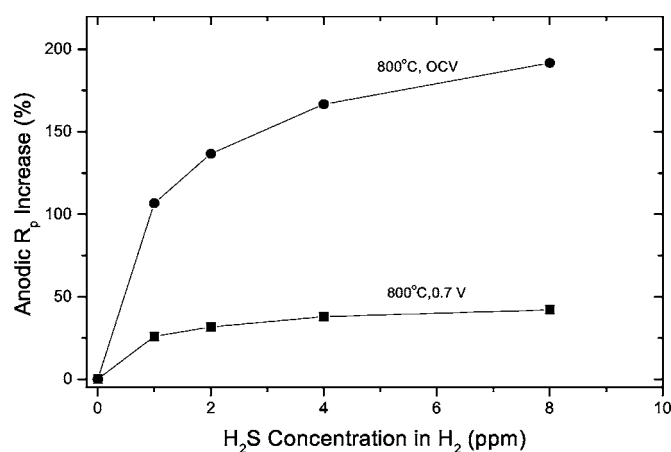


Figure 9. Changes in anodic polarization resistance (R_p) under OCV and at a cell voltage of 0.7 V at 800°C in fuels with different concentration of H_2S .

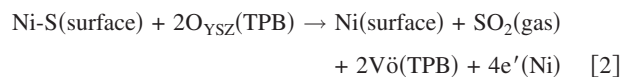
Proposed sulfur-Ni interaction mechanism.—Based on the poisoning behavior, we propose that the sulfur poisoning of Ni-based anode has two sequential stages dominated by different surface processes. The first stage is featured with a fast and dramatic degradation in performance, which is due most likely to surface sulfur adsorption. As soon as hydrogen sulfide touches the Ni surface, the following chemisorption occurs rapidly



As shown by both quantum chemical calculations and experimental proofs, sulfur absorbs strongly on Ni surfaces and hence blocks the active Ni sites for H_2 adsorption, dissociation, oxidation, and diffusion along surfaces.²⁴

The second stage of the sulfur poisoning is featured with slower degradation that lasts for days or even longer. The detailed mechanism for such a slow but continuous degradation is yet to be determined. One possible explanation is that, after the surface adsorption of sulfur on Ni reaches an equilibrium, continued sulfur exposure leads to surface reconstruction of nickel. Oliphant et al. found that surface reconstruction of Ni leading to new surfaces at intermediate H_2S concentrations (25–30 ppm $\text{H}_2\text{S}/\text{H}_2$) is favored for both supported and unsupported nickel.²⁹ Such a process is expected to be much slower than the surface adsorption process, and may cause a much slower degradation in fuel cell performance by changing the exposed crystal planes to less active ones. Some other explanation include possible interactions between sulfur and the electrolyte since Sasaki et al. showed Ni cermet anode with Sc_2O_3 stabilized ZrO_2 were much better than those with Y_2O_3 stabilized ZrO_2 in terms of sulfur tolerance.¹⁰ Further experiments are required to clarify on this point.

For the recovery process, from a thermodynamic point of view, Reaction 1 will be reversed when H_2S is removed from the feed, releasing the surface-adsorbed sulfur from the surface. After that, the subsurface sulfur atoms or ions will transfer to the outer nickel surface, followed by desorption from the nickel grain. Cell current may accelerate the regeneration (or de-sulfurization) process as follows



where O_{YSZ} represents a lattice oxygen, V_o an oxygen vacancy in YSZ, and TPB the triple-phase boundary between the electrode (Ni), electrolyte (YSZ), and the gas phase. The recovery may not be complete due probably to altered microstructure of the anode.

Conclusions

The performance of a Ni-YSZ anode in a real SOFC drops dramatically in minutes upon exposure to H_2S -containing fuel, followed by a gradual but steady degradation over days. The extent of sulfur poisoning increases with the concentration of H_2S in the fuel for a given operating temperature and cell voltage. For a given concentration of H_2S , the poisoning effect increased with decreasing cell operating temperature in the range of $700\text{--}900^\circ\text{C}$. Higher cell voltage (closer to OCV, under potentiostatic mode) leads to greater extent of sulfur poisoning in terms of performance drop. The degradation in performance can be recovered, at least partially, by switching from an H_2S -containing fuel to a clean fuel. Higher cell operating temperature and larger cell current density accelerated the recovery process, suggesting that the current passing through the cell might help the electrochemical oxidation of the sulfur adsorbed on anode surfaces.

Acknowledgment

This work was supported by Department of Energy, National Energy Technology Laboratory under the SECA Core Technology Program (grant no. DE-FC26-04NT42219).

Georgia Institute of Technology assisted in meeting the publication costs of this article.

References

1. E. P. Murray, T. Tsai, and S. A. Barnett, *Nature (London)*, **400**, 649 (1999).
2. S. Park, J. M. Vohs, and R. J. Gorte, *Nature (London)*, **404**, 265 (2000).
3. <http://www.netl.doe.gov/seca/>.
4. S. C. Singhal, R. J. Ruka, J. E. Bauerle, and C. J. Spengler, *Anode Development for Solid Oxide Fuel Cells, Final Technical Report*, DOE/MC/22046-2371, U.S. Department of Energy, Washington, DC, 1986.
5. D. Dees, U. Balachandran, S. Doris, J. Heiberger, C. McPheeter, and J. Picciolo, in *Solid Oxide Fuel Cells*, S. Singhal, Editor, PV 89-11, p. 317, The Electrochemical Society Proceedings Series, Pennington, NJ (1989).
6. J. Geyer, H. Kohlmuller, H. Landes, and R. Stubner, in *Solid Oxide Fuel Cells V*, U., Stimming, S. C. Singhal, H. Tagawa, W. Lennert, Editors, PV 97-40, p. 585, The Electrochemical Society Proceedings Series, Pennington, NJ (1997).
7. D. Stolten, R. Spah, and R. Schamm, in *Solid Oxide Fuel Cells V*, U., Stimming, S. C. Singhal, H. Tagawa, W. Lennert, Editors, PV 97-40, p. 88, The Electrochemical Society Proceedings Series, Pennington, NJ (1997).
8. Y. Matsuzaki and I. Yasuda, *Solid State Ionics*, **132**, 261 (2000).
9. A. L. Dicks, *J. Power Sources*, **61**, 113 (1996).
10. K. Sasaki, K. Susuki, A. Iyoshi, M. Uchimura, N. Imamura, H. Kusaba, Y. Teraoka, H. Fuchino, K. Tsujimoto, Y. Uchida, and N. Jingo, in *Solid Oxide Fuel Cells IX*, S. C. Singhal, and J. Mizusaki, Editors, PV 2005-07, p. 1267, The Electrochemical Society Proceedings Series, Pennington, NJ (2005).
11. S. J. Xia and V. I. Birss, in *Solid Oxide Fuel Cells IX*, S. C. Singhal, and J. Mizusaki, Editors, PV 2005-07, p. 1275, The Electrochemical Society Proceedings Series, Pennington, NJ (2005).
12. N. U. Pujare, K. W. Semkow, and A. F. Sammells, *J. Electrochem. Soc.*, **134**, 2639 (1987).
13. C. Yates and J. Winnick, *J. Electrochem. Soc.*, **146**, 2841 (1999).
14. M. Liu, G. Wei, J. Luo, A. R. Sanger, and K. T. Chung, *J. Electrochem. Soc.*, **150**, A1025 (2003).
15. R. Mukundan, E. L. Brosha, and F. H. Garzon, *Electrochem. Solid-State Lett.*, **7**, A5 (2004).
16. L. Aguilar, S. Zha, Z. Cheng, J. Winnick, and M. Liu, *J. Power Sources*, **135**, 17 (2004).
17. H. P. He, R. J. Gorte, and J. M. Vohs, *Electrochem. Solid-State Lett.*, **8**, A279 (2005).
18. S. Zha, P. Tsang, Z. Cheng, and M. Liu, *J. Solid State Chem.*, **178**, 1847 (2005).
19. S. Zha, Z. Cheng, and M. Liu, *Electrochem. Solid-State Lett.*, **8**, A406 (2005).
20. Z. Cheng, S. Zha, L. Aguilar, D. Wang, J. Winnick, and M. Liu, *Electrochem. Solid-State Lett.*, **9**, A31 (2006).
21. Y. H. Huang, R. I. Dass, Z. L. Xing, and J. B. Goodenough, *Science*, **312**, 254 (2006).
22. T. Rosenqvist, *J. Iron Steel Inst., London*, **176**, 37 (1954).
23. Z. Cheng, S. Zha, and M. Liu, *J. Electrochem. Soc.*, **153**, A1302 (2006).
24. C. H. Bartholomew, P. K. Agrawal, and J. R. Katzer, *Adv. Catal.*, **31**, 135 (1982).
25. S. P. Simner, M. D. Anderson, L. R. Pederson, and J. W. Stevenson, *J. Electrochem. Soc.*, **152**, A1851 (2005).
26. Y.-K. Lee, J.-Y. Kim, Y.-K. Lee, I. Kim, H.-S. Moon, J.-W. Park, C. P. Jacobson, and S. J. Visco, *J. Power Sources*, **115**, 219 (2003).
27. S. P. Jiang, J. G. Love, J. P. Zhang, M. Hoang, Y. Ramprakash, A. E. Hughes, and S. P. S. Badwal, *Solid State Ionics*, **121**, 1 (1999).
28. M. J. Jorgensen and M. Mogensen, *J. Electrochem. Soc.*, **148**, A433 (2001).
29. J. L. Oliphant, R. W. Fower, R. B. Pannell, and C. H. Bartholomew, *J. Catal.*, **51**, 229 (1978).